Journal of Drug Targeting

http://informahealthcare.com/drt
ISSN: 1061-186X (print), 1029-2330 (electronic)

J Drug Target, 2014; 22(7): 658–668
 DOI: 10.3109/1061186X.2014.928718

informa
healthcare

ORIGINAL ARTICLE

A medusa-like β-cyclodextrin with 1-methyl-2-(2′-carboxyethyl) maleic anhydrides, a potential carrier for pH-sensitive drug delivery

Sunyoung Kang[1], Euddeum Park[1], Youngeun Kim[1], Seonju Lee[1], Jiwoong Kwon[2], Hyungdo Cho[1], and Yan Lee[1]

[1]*Department of Chemistry and* [2]*WCU Department of Biophysics and Chemical Biology, College of Natural Sciences, Seoul National University, Seoul, Republic of Korea*

Abstract

We developed a new pH-sensitive drug delivery carrier based on β-cyclodextrin (β-CD) and 1-methyl-2-(2′-carboxyethyl) maleic anhydrides (MCM). The primary hydroxyl groups of β-CD were successfully attached to MCM residues to produce a medusa-like β-CD–MCM. The MCM residue was conjugated with cephradine (CP) with high efficiency (>90%). More importantly, β-CD–MCM–CP responded to the small pH drop from 7.4 to 5.5 and released greater than 80% of the drugs within 0.5 h at pH 5.5. In addition, the inclusion complex between β-CD–MCM–CP and the adamantane derivative was formed by simple mixing to show the possibility of introducing multi-functionality. Based on these results, β-CD–MCM can target weakly acidic tissues or organelles, such as tumours, inflammatory tissues, abscesses or endosomes, and be easily modified with various functional moieties, such as ligands for cell binding or penetration, enabling more efficient and specific drug delivery.

Keywords

Acidic environment, cephradine, dimethylmaleic acid anhydride, drug conjugation

History

Received 1 April 2014
Revised 14 May 2014
Accepted 22 May 2014
Published online 23 June 2014

Introduction

For efficient and safe delivery of drugs to specific targets, smart drug delivery techniques have evolved along with the development of various signal-responsive materials [1–3]. Abrupt changes in the physicochemical properties of smart materials in response to physical signals such as temperature [4] and light [5] as well as chemical signals such as pH [6], glutathione [7], and enzymes [8] can induce encapsulation and release of drugs in specific conditions. Among these, pH has been frequently selected as the controlling trigger because the pH value can represent a certain physiological condition in many target sites in the body. The pH variation through the gastrointestinal tract has been used for the site-specific drug delivery to strongly acidic stomach or weakly alkaline small intestine [9]. Enhanced glycolysis in cancer tissues lowers the pH to 5–6, and similar pH lowering is also observed in inflammatory tissues [10] and abscesses [11,12]. The weakly acidic pH value is recognised as an inducing signal for the release of anti-cancer [13] or anti-inflammatory drugs [14]. Moreover, the early endosomal pH value of 5–6 is frequently used as the signal for the endosomal escape of macromolecular drugs such as pDNA [15], siRNA [16] or proteins [17], which have difficulty penetrating the cell membrane and should be delivered into the cell interior *via* an endocytic pathway [18]. However, smart materials with rapid degradability responding to small pH variations are still under active investigation for a more practical drug delivery system because the pH variation in the human body is not extreme, with a few exceptions.

As a chemical moiety for pH-responsive smart materials, maleic acid amide derivatives are attractive owing to their rapid degradability at an appropriate pH. Unlike other amides, which can only be degraded at extreme pH conditions, maleic acid amide derivatives can be degraded within a biologically tolerable pH range [19]. The responsive pH range and the degradation rate can be finely tuned by a change of alkyl substituents on the *cis*-double bonds [20]. Moreover, the maleic acid amide derivatives can be synthesised *via* the one-step ring-opening reaction between amines and corresponding maleic acid anhydride derivatives under weakly alkaline conditions. The easy synthesis of maleic acid amide derivatives under mild conditions is a strong advantage over other pH-sensitive linkages, which require quite complicated synthetic steps in conjugation of drugs or cross-linking of carrier backbones [21].

In this study, we wanted to synthesise a drug carrier based on 1-methyl-2-(2′-carboxyethyl) maleic anhydride (MCM) or carboxylate dimethyl maleic anhydride (CDM), a maleic acid anhydride derivative with two alkyl substituents. Because the acid amide correspondent from MCM is stable at normal physiological pH 7.4 but rapidly degradable at pH 5.5 [22], an MCM derivative might be one of the best candidates for the conjugation with drugs targeting weakly acidic

Address for correspondence: Yan Lee, Department of Chemistry, College of Natural Sciences, Seoul National University, Gwanak-ro 1, Gwanak-gu, Seoul 151-747, Republic of Korea. Tel: +82 2 880 4344. Fax: +82 2 871 2496. E-mail: gacn@snu.ac.kr

environments. We designed a drug carrier with several MCM residues on the surface for the easiest conjugation with amine-based drugs or cross-linkers.

As the backbone of the drug carrier, we selected β-cyclodextrin (β-CD), a cyclic oligosaccharide with seven glucose molecules. β-Cyclodextrin (β-CD) has been widely used as a part of drug delivery carrier due to its high biocompatibility [23]. Many functional groups can be readily introduced into the β-CD backbone because it has 7 primary and 14 secondary hydroxyl groups. A medusa-like structure can be synthesised by reaction with the seven primary hydroxyl groups [24]. The regioselective functionalization of β-CD enables to achieve homogeneous chemical properties of the conjugated functional moieties. Furthermore, the toroidal interior of β-CD can be used for the introduction of additional functionality such as a targeting ligand [25] or cell-penetrating moiety [26] by host–guest inclusion because the interior can strongly interact with small hydrophobic molecules such as adamantane *via* non-covalent interactions [27]. Polymers or nanoparticles with adamantane moieties can be easily modified with β-CD derivatives by the host–guest interaction [28].

We expected that the medusa-like β-CD could be conjugated with drug molecules *via* pH-sensitive MCM linkers by simple mixing in mildly alkaline conditions and that other functional moieties with adamantane residues could also be non-covalently introduced into the pore of the β-CD. Otherwise, the surface of other drug carriers such as polymers or nanoparticles can be non-covalently modified with the pH-sensitive medusa-like β-CD derivative. The resulting carrier could rapidly release the conjugated drugs in weakly acidic conditions. The general conceptual scheme is illustrated in Figure 1. By using cephradine (CP), a cephalosporin antibiotic, as a drug to be targeted to weakly acidic inflammatory tissues, we wanted to prove our concept *in vitro*. The medusa-like β-CD derivatives has strong potential for multi-functional drug delivery systems for targeting tumours, inflammatory tissues or abscesses as well as for the rapid response at the pH of early endosomes in intracellular drug delivery.

Materials and methods

Materials

CP was obtained from Han Wha Pharm. Co., Ltd. (Seoul, South Korea). β-CD, 6-aminohexanoic acid, di-*tert*-butyl dicarbonate ($(Boc)_2O$), *n*-butylamine (BA), triethylamine (TEA), diisopropylethylamine (DIPEA), diisopropylcarbodiimide (DIC), 4-dimethylaminopyridine (DMAP), *p*-toluenesulphonic acid (PTSA), trifluoroacetic acid (TFA), sodium hydride (NaH) (60% in mineral oil), *N,N,N′,N′*-tetramethyl-*O*-(1*H*-benzotriazol-1-yl)uronium hexafluorophosphate (HBTU), fluorescein isothiocyanate (FITC) isomer I and dimethylsulphoxide (DMSO) were purchased from Sigma-Aldrich (St Louis, MO). Triethyl-2-phosphonopropionate, dimethyl-2-oxoglutarate and 1-adamantaneamine hydrochloride were purchased from TCI (Tokyo, Japan). Ammonium chloride (NH_4Cl), magnesium sulphate ($MgSO_4$), potassium hydroxide (KOH), sodium chloride (NaCl), sodium hydroxide (NaOH), sodium bicarbonate ($NaHCO_3$), tetrahydrofuran (THF), dimethylformamide (DMF), hexane, ethyl acetate (EA), methanol (MeOH), ethanol, dichloromethane (DCM), hydrochloric acid (HCl), acetonitrile (ACN) and pyridine were purchased from Daejung (Seoul, South Korea). Anhydrous TEA, THF and DMF were obtained by distillation of the reagent-grade materials. Other reagents were used without further purification.

Synthesis

Synthesis of compound 1. Following the method described in a previous report [29], compound 1 was prepared. Briefly, NaH (0.37 g, 9.2 mmol) was added slowly into a solution of triethyl-2-phosphonopropionate (1.64 g, 6.89 mmol) in anhydrous THF (30 mL) at 0 °C under a nitrogen atmosphere. Dimethyl-2-oxoglutarate (1.00 g, 5.74 mmol) was added to the solution after the evolution of hydrogen gas had stopped. The reaction mixture was further stirred while maintaining the temperature at 0 °C. After the reaction completion was confirmed by TLC, a saturated aqueous solution of NH_4Cl was added dropwise. Following the removal of THF by rotary

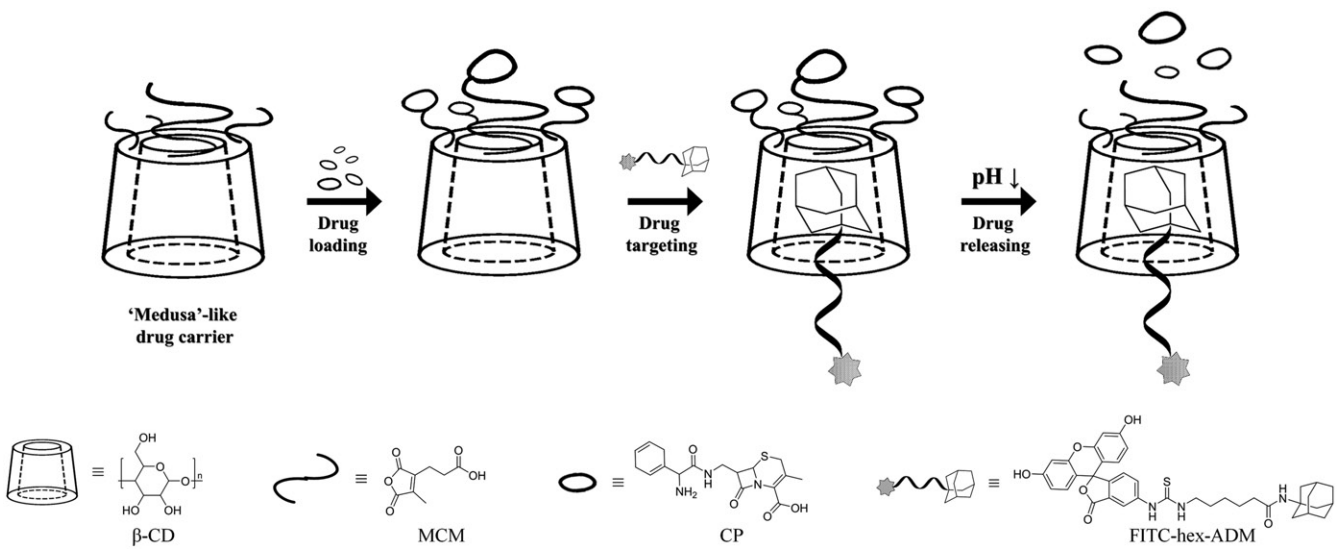

Figure 1. General scheme of pH-sensitive drug delivery by a medusa-like β-CD–MCM.

evaporation, the resulting solid and water mixture was extracted with EA several times. The organic phase was combined, washed with deionised water (DIW) and brine, dried over $MgSO_4$ and concentrated by rotary evaporation. The residue was purified by silica gel chromatography eluted with EA/hexane to yield compound 1 as a colourless oil. Yield: 91%, ^{1}H NMR (300 MHz, $CDCl_3$): δ 1.25–1.30 (3H, t, C*H*$_3$CH$_2$O), 1.98 (3H, s, C*H*$_3$C), 2.46–2.49 (2H, m, CC*H*$_2$CH$_2$), 2.62–2.65 (2H, m, CH$_2$C*H*$_2$CO), 3.66 (3H, s, CO$_2$C*H*$_3$), 3.73 (3H, s, C*H*$_3$O$_2$CC) and 4.16–4.22 (2H, q, CH$_3$C*H*$_2$O).

Synthesis of compound 2. Following the method described in a previous report [29], compound 2 was prepared. Briefly, compound 1 in a 2 M KOH solution in ethanol was allowed to reflux for 1 h. DIW was added, and the hot reaction mixture was cooled to ambient temperature. After removal of ethanol by evaporation, the aqueous phase was washed with DCM several times and acidified to pH 2 using concentrated HCl. The aqueous phase was then extracted with EA several times. The organic phase was dried over $MgSO_4$ and concentrated under reduced pressure to produce MCM (2) as a white solid. Yield: 74%, ^{1}H NMR (300 MHz, $CDCl_3$): δ 2.12 (3H, s, CC*H*$_3$) and 2.77 (4H, s, CC*H*$_2$C*H*$_2$CO).

Synthesis of compound 3. To a solution of compound 2 (2.00 g, 1.09 mmol), β-CD (0.10 g, 0.092 mmol), DMAP (0.46 g, 0.37 mmol) and PTSA (0.70 g, 0.37 mmol) in DMF (10 mL) was added DIC (0.33 g, 2.6 mmol). The reaction mixture was stirred overnight at ambient temperature. The crude product was purified by dialysis with regenerated cellulose membrane (MWCO 1000, SPECTRUM®) in phosphate buffer (pH 9.0), HCl solution (pH 3.0) and DIW, respectively. Lyophilisation was performed next. An off-white power, β-CD–MCM (3) was obtained. Yield: 85%, ^{1}H NMR (300 MHz, 1.1 wt% NaOD in D_2O): δ 1.65 (3H, s, CC*H*$_3$), 1.98–2.10 (2H, m, CC*H*$_2$CH$_2$), 2.21–2.33 (2H, m, CH$_2$C*H*$_2$CO), 3.26–3.36 (2H, m, 2′, 4′-C*H*-β-CD), 3.67–3.80 (4H, m, 3′, 5′-C*H*, 6′-C*H*$_2$-β-CD), 4.94 (1H, s, 1′-C*H*-β-CD) (Figure 3a); matrix-assisted laser desorption ionization-time of flight (MALDI-TOF) (m/z): 1490, 1656, 1882, 1988, 2155 and 2321 $[M+Na]^+$ (Figure 3b).

Synthesis of compound 4. A solution of 3 (0.050 g, 0.024 mmol) in ACN (5 mL) was added with excess TEA at ambient temperature and stirred until becoming a completely clear solution. BA (0.24 mL, 0.242 mmol) was added dropwise into the reaction mixture. After overnight stirring, the reaction mixture was evaporated to remove the solvents. A 1 M NaOH solution (12 equiv.) was added carefully to the aqueous solution of compound 4 to exchange excess *n*-butylammonium cations with sodium cations. The aqueous crude was evaporated and dried in vacuum, and then a light brown powder, β-CD–MCM–BA (4), was obtained. Yield: > 90%, ^{1}H NMR (300 MHz, 1.1 wt% NaOD in D_2O): δ 0.89–0.94 (3H, t, C*H*3CH2), 1.32–1.39 (2H, m, CH3C*H*2CH2), 1.46–1.54 (2H, m, CH2C*H*2CH2), 1.87 (3H, s, CC*H*3), 2.22–2.31 (2H, m, CH2C*H*3CO), 2.49–2.56 (2H, m, CC*H*2CH2), 3.18–3.23 (2H, m, CH2C*H*2NH), 3.54–3.63 (2H, m, 2′, 4′-C*H*-β-CD), 3.65–3.92 (4H, m, 3′, 5′-C*H*, 6′-C*H*$_2$-β-CD), 5.05 (1H, s, 1H, s, 1′-C*H*-β-CD).

Synthesis of compound 5. β-CD–MCM–CP (5) was synthesised employing the same preparation method as used for compound 4, but using CP solution (6 equiv.) in ACN instead of BA. After purification, yellow solid was obtained. Yield: > 90%, ^{1}H NMR (300 MHz, 1.1 wt% NaOD in D_2O): δ 1.83 (3H, s, C*H*$_3$-cephalosporin), 1.86 (3H, s, CC*H*$_3$), 2.18–2.24 (2H, m, CC*H*$_2$H$_2$), 2.45–2.48 (2H, m, CH$_2$C*H*$_2$CO), 2.62–2.71 (4H, m, 3′, 6′-C*H*$_2$-cyclohexadiene), 2.99–3.08 (1H, m, SC*H*$_2$C-cephalosporin), 3.12–3.18 (1H, m, SC*H*$_2$C-cephalosporin), 3.39–3.49 (2H, m, 2′, 4′-C*H*-β-CD), 3.77–3.83 (4H, m, 3′, 5′-C*H*, 6′-C*H*$_2$-β-CD), 4.73 (1H, s, 1′-CC*H*-cyclohexadiene), 4.87 (1H, s, NC*H*S), 4.90 (1H, s, 1′-C*H*-β-CD), 5.71–5.73 (3H, m, NHC*H*CO, 4′, 5′-C*H*-cyclohexadiene), 5.87 (1H, s, 2′-C*H*-cyclohexadiene).

Synthesis of compound 6. 6-Aminohexanoic acid (1.00 g, 7.26 mmol) was dissolved in the co-solvent of THF:aqueous saturated $NaHCO_3$ solution (1:1) and a solution of di-*tert*-butyl dicarbonate (2.00 g, 9.15 mmol) in THF was added dropwise into the solution at ambient temperature. After the reaction completion was confirmed by TLC, following the removal of THF by rotary evaporation and the resulting solution was acidified down to pH 1–2. The mixture was extracted with DCM several times. The organic phase was combined, washed with deionised brine, dried over $MgSO_4$ and concentrated by rotary evaporation. The pure compound, *N*-Boc-aminohexanoic acid (6) was obtained as an opaque crystal. Yield: 81%, ^{1}H NMR (300 MHz, 1.1 wt% NaOD in D_2O): δ 1.10–1.28 (2H, m, CH$_2$C*H*$_2$CH$_2$), 1.32–1.56 (13H, m, CH$_2$C*H*$_2$CH$_2$C*H*$_2$CH$_2$, *t*-Boc), 2.10–2.15 (2H, t, CH$_2$C*H*$_2$CO$_2$H) and 2.99–3.03 (2H, t, NHC*H*$_2$CH$_2$).

Synthesis of compound 7. Following the method described in a previous report [30], compound 7 was prepared. Briefly, a solution of compound 6 (0.10 g, 0.43 mmol) and 1-adamantaneamine hydrochloride (0.080 g, 0.43 mmol) in dry THF (9 mL) was treated with DIPEA (0.12 mL, 0.86 mmol) and HBTU (0.16 g, 0.43 mmol). After being stirred for 16 h at room temperature, the reaction mixture was heated at 60 °C for 90 min. Then, DCM and brine were added, and the organic phase was washed twice with 1 M aqueous HCl (10 mL), twice with 5% aqueous $NaHCO_3$ (10 mL) and twice with brine (10 mL), and then dried over Na_2SO_4. The residue was purified by silica gel chromatography eluted with EA/hexane to yield compound 7 as a white solid. Yield: 54%, ^{1}H NMR (300 MHz, $CDCl_3$): δ 1.27–1.35 (2H, m, CH$_2$C*H*$_2$CH2), 1.42–1.49 (11H, s, m, t-Boc, C*H*$_2$CH$_2$CO), 1.55–1.59 (2H, m, NHCH$_2$C*H*$_2$), 1.61–1.65 (6H, br, CC*H*$_2$CH-ADM), 1.89–1.97 (6H, br, CHC*H*$_2$CH-ADM), 2.03–2.08 (5H, m, CH$_2$C*H*CH$_2$-ADM, CH$_2$C*H*$_2$CO) and 3.08–3.14 (2H, m, NHC*H*$_2$CH$_2$).

Synthesis of compound 8. Excess TFA (10 mL) was added to compound 7 (0.75 g, 2.1 mmol) in DCM (30 mL) at 0 °C. The solution was stirred for 2 h, concentrated, washed with saturated $NaHCO_3$ and brine, and dried over MgSO4. Compound 8 was obtained as a white solid without further purification. Yield: 89%, ^{1}H NMR (300 MHz, 1.2 wt% DCl in D_2O): δ 1.16–1.26 (2H, m, CH$_2$C*H*$_2$CH$_2$), 1.40–1.56 (10H, m, C*H*$_2$CH$_2$C*H*$_2$, CC*H*$_2$CH-ADM), 1.81 (6H, br, CHC*H*$_2$CH-ADM), 1.89 (3H, br, CH$_2$C*H*CH$_2$-ADM), 2.04–2.09 (2H, t, CH$_2$C*H*$_2$CO) and 2.80–2.85 (2H, t, NH$_2$C*H*$_2$CH$_2$).

Synthesis of compound 9. FITC isomer 1 (0.04 mg, 0.113 mmol) was added in a solution of compound 8 (0.030 g, 0.11 mmol) in MeOH (5 mL), followed by saturated $NaHCO_3$ (1 mL). After stirring overnight, the reaction

mixture was purified by reverse-phase high-performance liquid chromatography (HPLC) with a linear gradient over 30 min from 50 to 100% of ACN/DIW with 0.1% TFA at a flow rate of 6 mL/min. Compound 9 was obtained as an orange solid. Yield: 32%, ^{1}H NMR (300 MHz, MeOD): δ 1.40–1.45 (2H, m, $CH_2CH_2CH_2$), 1.61–1.66 (2H, m, CH_2CH_2CO), 1.69–1.73 (8H, s, m, CCH_2CH-ADM, $NHCH_2CH_2$), 2.01 (9H, br, $CHCH_2CH$-ADM, CH_2CHCH_2-ADM), 2.13–2.16 (2H, t, CH_2CH_2CO), 3.65 (2H, br, $NHCH_2CH_2$), 6.55 (2H, s, 2′-C*H*-xanthene), 6.56–6.58 (2H, dd, 4′-C*H*-xanthene), 7.17–7.19 (2H, d, 5′-C*H*-xanthene), 7.20–7.22 (1H, d, 4′-C*H*-isobenzofuranone), 7.62–7.64 (1H, d, 5′-C*H*- isobenzofuranone), 7.82 (1H, s, 7′-C*H*-isobenzofuranone).

Measurement of pH-sensitive drug release

Release of BA from β-CD–MCM–BA

pH-sensitive release of BA from β-CD–MCM–BA (4) was confirmed by ^{1}H NMR. β-CD–MCM–BA was dissolved in 1.2 wt% DCl at the concentration of 3 mg/mL. After incubation with stirring at 37 °C for 8 h, ^{1}H NMR was measured by a Bruker Avance DPX-300 (Germany) (Figure 4).

Release of CP from β-CD–MCM–CP

β-CD–MCM–CP (5) was dissolved in a pH 7.4 phosphate buffer (100 mM) or a pH 5.5 acetate buffer (100 mM) at a concentration of 3 mg/mL, and each solution was incubated with stirring at 37 °C. A YOUNGLIN HPLC (9000 HPLC, South Korea) equipped with a UV detector and a reverse-phase column (Agilent Eclipse XDB-C18 4.6×150 mm, 5 μm) was used for the HPLC-based measurement. At various time points, each sample was collected and diluted 10 times with the same buffer. After filtering through a 0.2-μm polyvinylidene fluoride syringe filter, the sample was injected into the HPLC system. A mixture (3:7 v/v) of MeOH:pH 9.0 phosphate buffer (50 mM) was used as the eluent, and the flow rate was set at 0.5 mL/min. The release of CP was measured by UV absorbance at wavelengths 245 and 270 nm (Figure 5).

Complex formation between compound 5 and 9

Fluorescence correlation spectroscopy measurement

A home-built fluorescence confocal microscope setup was used to measure the autocorrelation of the fluorescent probe, FITC. A 488-nm continuous blue laser diode (TECBL-20GC-488, World Star Tech, Toronto, Canada) was coupled with a single-mode optical fibre ($\Phi = 3$–5 μm, P1-488-PM-FC, Thorlabs, Newton, NJ) for the beam clean-up and illuminated the sample through a water-immersion objective (NA = 1.20, $60\times$, f = 3 mm, Olympus, Tokyo, Japan) mounted in a homemade microscope body. The fluorescence signal was distinguished with the excitation light by a dichroic mirror (ZT488rdc, Chroma, Bellows Falls, VT) and further cleaned by an emission filter (HQ525/50 m, Chroma). A 1:2 multi-mode fibre optic coupler (($\Phi = 62.5$ μm, FCMM625-50A-FC) was used as a pinhole to reduce the background from the focal volume, and two avalanche photodiodes (SPCM-AQR-14-FC, Perkin Elmer, Waltham, MA) collected the fluorescence signals. The correlation was measured with a correlator card (FLEX02-01D, Correlator.com) and further analysed by a homemade analysis program coded with LabVIEW 2009 (National Instruments, Austin, TX).

The fluorescence correlation spectroscopy (FCS) setup was calibrated to determine the axial and lateral dimensions of the confocal volume by using a fluorophore, Alexa 488, whose diffusion coefficient is $D = 4.35 \times 10^{-6}$ cm^2/s [31]. The process followed the procedure described in reference [32]. Calibration showed that the lateral $1/e^2$ dimension was 232 nm with the aspect ratio of 7.18, indicating that the measured focal volume was 0.501 fL.

For the measurement of complex formation, a solution of compound 9 (10 nM) in pH 9.0 phosphate buffer (50 mM) was prepared with different concentrations of compound 5. Bovine serum albumin was added to the mixture at the final concentration of 0.1 mg/mL to prevent the nonspecific binding between compounds 5 and 9. Each correlation curve was measured six times for 10 min each (once for each concentration of compound 5) to suppress the thermal noises and background signals.

Rotating frame overhauser effect spectroscopy

The complex between β-CD and compound 9 and the complex between β-CD–MCM–CP (compound 5) and compound 9 were prepared by mixing at a 1:1 molar ratio at a concentration of 3 mM in a D_2O-based pH 9.0 phosphate buffer (50 mM). NMR spectra recorded at 25 °C on a Agilent Technologies 400-MR DD2 (Santa Clara, CA) spectrometer. Rotating frame overhauser effect spectroscopy (ROESY) experiment was performed using the standard protocols contained in the spectrometer library (mixing time: 300 ms; T_1 experiment).

Cytotoxicity

Cell viability was measured by 3-(4,5-dimethylthiazol-2-yl)-2,5-diphenyltetrazolium bromide (MTT; Sigma-Aldrich) assay. NIH-3T3 cells (mouse embryonic fibroblast cell line) were seeded at 5.0×10^3 cells/well in a 96-well plate in 90 μL of Dulbecco's modified eagle's medium WelGene containing 10% foetal bovine serum; WelGene (Daegu, South Korea) and incubated at 37 °C for 24 h. To determine the cytotoxicity, 10 μL of the solution of each sample with various concentrations was added into the media with subsequent incubation at 37 °C for 48 h. For the assay, the cells were washed with Dulbecco's phosphate-buffered saline (DPBS; WelGene), followed by the addition of 20 μL of filtered MTT solution (2 mg/mL in DPBS). After incubation at 37 °C for 2 h, the medium was removed from the well, and 150 μL of DMSO was added to dissolve the insoluble formazan particles. The absorbance was measured at 570 nm using a microplate reader (Molecular Devices Co., Menlo Park, CA). The relative cell viability (%) was defined as the percentage of viable cells compared with the same percentage in the control (cells treated with DPBS solution).

Results

Synthesis of β-CD–MCM

We synthesised a pH-sensitive drug carrier based on β-CD and MCM for efficient drug conjugation, rapid drug release at

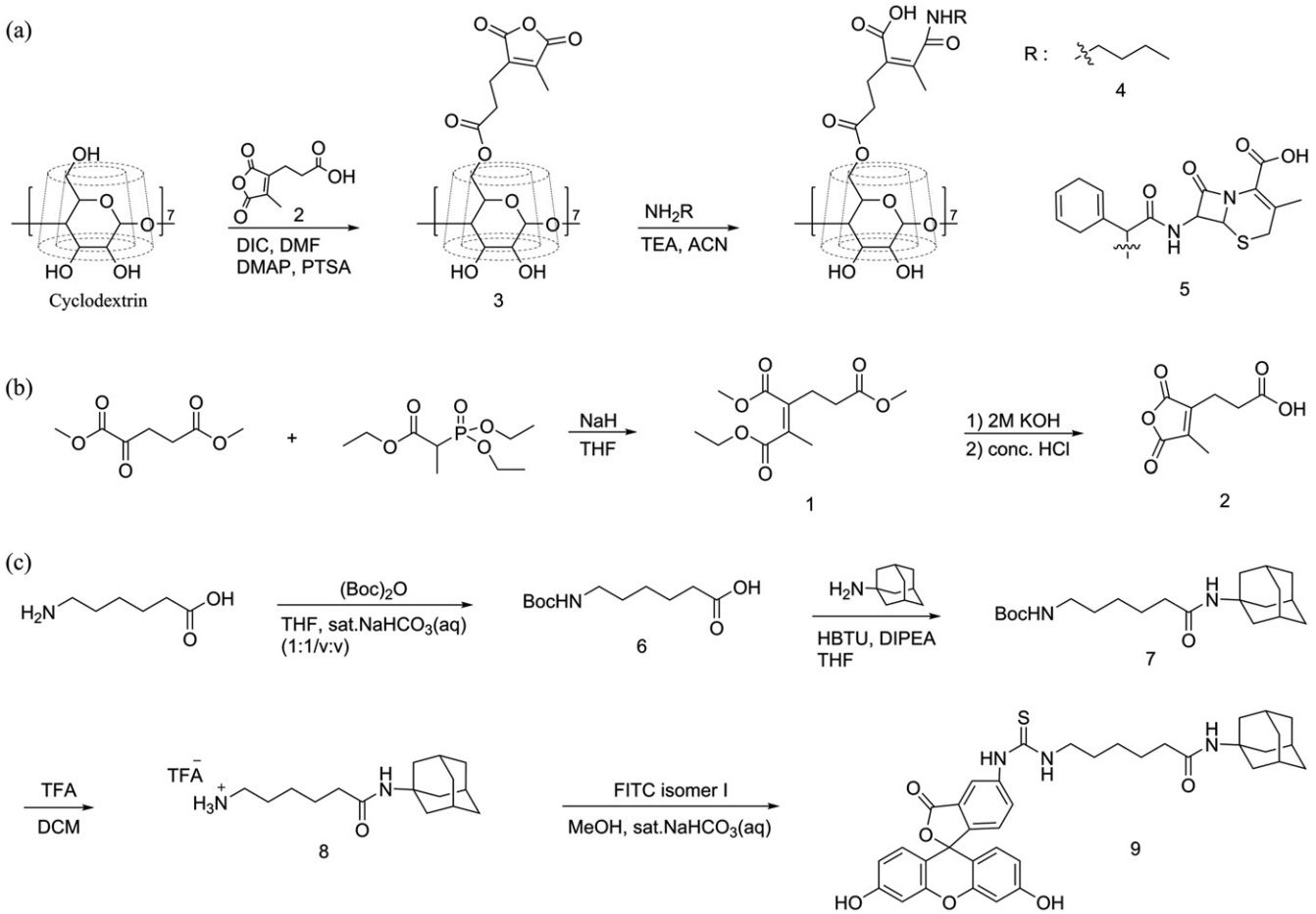

Figure 2. Synthetic schemes of β-CD–MCM and its drug conjugate. (a) Synthesis of β-CD–MCM–BA and β-CD–MCM–CP, (b) Synthesis of 1-methyl-2-(2′-carboxyethyl) maleic anhydride (MCM) and (c) synthesis of FITC-hex-ADM.

acidic pH and simple introduction of functional ligands. The synthetic scheme is shown in Figure 2(a). After the synthesis of MCM by the Horner–Wadsworth–Emmons reaction between triethyl-2-phosphonopropionate and dimethyl-2-oxoglutarate (Figure 2b) [29], MCM was coupled with the β-CD molecule *via* the formation of ester bond between the carboxyl group of MCM and the hydroxyl group of β-CD. A β-CD molecule has seven primary hydroxyl groups and fourteen secondary hydroxyl groups. Among them, primary hydroxyl groups at the 6′-C position of the glucose are more reactive to electrophiles, and they preferably react with the carboxyl group using a carbodiimide-coupling reagent, DIC. β-CD–MCM was purified from the excess reagents by dialysis.

The formation of β-CD–MCM was confirmed by ^{1}H NMR and MALDI-TOF mass spectrometry (Figure 3). The numbers of MCM residues per a β-CD–MCM molecule was calculated to be six by ^{1}H NMR. In other words, 85% of primary hydroxyl groups of β-CD were conjugated with MCM on average. The MALDI-TOF mass spectra exhibited the presence of β-CD–MCM molecules with various numbers of MCM residues: β-CD–$(MCM)_2$ (1490), β-CD–$(MCM)_3$ (1656), β-CD–$(MCM)_4$ (1822), β-CD–$(MCM)_5$ (1988), β-CD–$(MCM)_6$ (2154) and β-CD–$(MCM)_7$ (2322). Considering the average conjugation number was six by ^{1}H NMR and the main peak of the MALDI-TOF spectra was that of β-CD–$(MCM)_4$, the MALDI-TOF spectra could not represent the distribution of various β-CD–(MCM) molecules accurately, most likely due to the different ionisation degrees of the β-CD–(MCM) variants.

Drug conjugation with β-CD–MCM

At first, a simple primary amine, BA, was used as a model drug for the optimisation of the conjugation reaction. By simple mixing in a weakly basic condition, BA was successfully introduced into β-CD–MCM. The ^{1}H NMR spectrum shows the formation of the acid amide linkage between BA and β-CD–MCM (Figure 4). Greater than 90% of MCM moieties in β-CD–MCM were reacted with BA, and only a small amount of unreacted BA were remained.

Then, CP, an amine-containing antibiotic drug, was conjugated with β-CD–MCM by a similar method. The formation of β-CD–MCM–CP was confirmed by both ^{1}H NMR and HPLC. The amount of CP with a strong UV absorption was easily analysed by a UV detector. High conjugation efficiency ($92.5 \pm 2.5\%$) was observed in the formation of β-CD–MCM–CP. As we applied six equivalents of CP to β-CD–MCM with six MCM moieties, nearly exhaustive conjugation was accomplished by the simple mixing. In addition, the drug content in β-CD–MCM–CP was calculated to be $28 \pm 5.5\%$ by comparing the mass of CP and the total mass of β-CD–MCM–CP with some residual sodium and TEA salts.

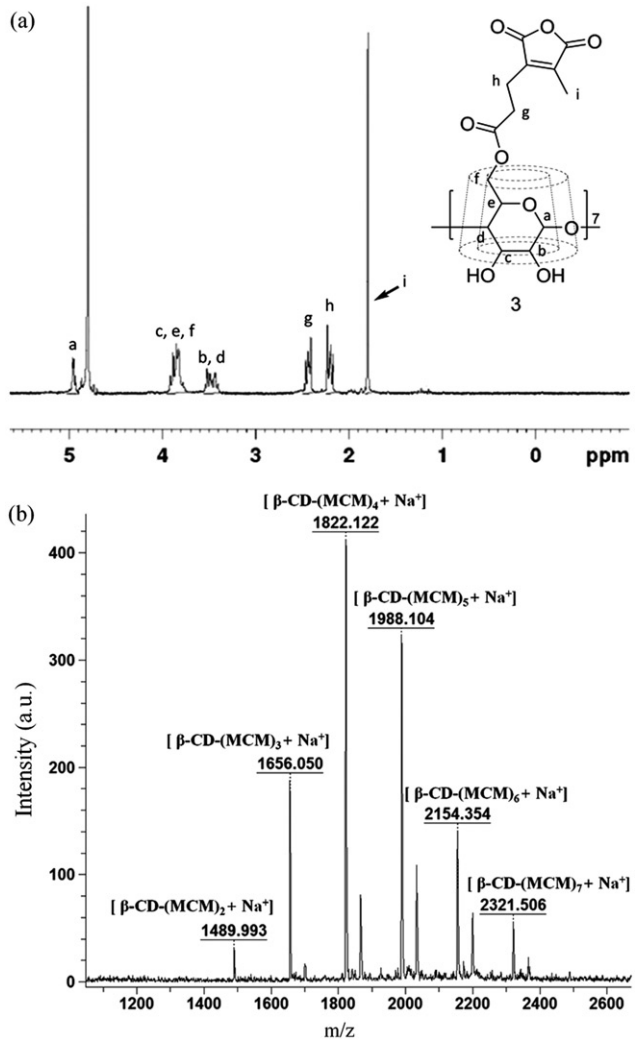

Figure 3. Confirmation of synthesis of β-CD–MCM. (a) ^{1}H NMR (NMR solvent: D_2O) and (b) MALDI-TOF spectra of β-CD–MCM.

pH-sensitive drug release

The pH-sensitive degradation of the MCM acid amide bond was investigated by ^{1}H NMR. The methylene protons (marked with x) next to the nitrogen in the intact amide of β-CD–MCM–BA showed a peak at 3.18–3.23 ppm, while the peak (marked with *) was shifted to 2.55–2.62 ppm, equal to the methylene peak of free BA, in an acidic solution (1.2 wt% DCl in D2O) (Figure 4). The chemical shift confirmed the degradation of the MCM acid amide and the release of conjugated BA.

Cumulative release of CP from β-CD–MCM–CP at pH 5.5 and pH 7.4 was measured by HPLC to determine the degradation kinetics in more detail (Figure 5). At pH 7.4, less than 20% of CP was released from β-CD–MCM–CP, even after 5 h. On the other hand, a rapid burst of CP was observed at pH 5.5, and more than 80% of CP was released within 0.5 h. The release was almost completed at approximately 95% in 1 h. A dramatic difference in release kinetics was observed between pH 5.5 and pH 7.4. In addition, we confirmed the stability of CP during the conjugation and release procedure. The ^{1}H NMR spectrum of the CP released from β-CD–MCM–CP at pH 5.5 was identical to that of the initial CP (Figure 6a). The mass spectra of the two CPs obtained by electrospray ionisation were also identical (350.1 $[M+H]^+$ and 699.1 $[M+M]^+$, Figure 6b). Based on these data, we believe that CP was quite stable during the conjugation in mildly basic conditions and during the release in weakly acidic conditions.

Complex formation between β-CD–MCM–CP and the adamantane derivative

To clarify the formation of the complex between the β-CD-based drug conjugate and an adamantane derivative, we used FCS, which analyses the variation in the diffusion coefficient of a fluorophore attached to guest or host [33]. FITC was conjugated to the adamantane derivative [34] as a probe (FITC-hex-ADM) (Figure 2c). The average diffusion time of the fluorophore was measured with varying the concentration of the host molecule, β-CD–MCM–CP. As the concentration of β-CD–MCM–CP increased, the average diffusion time also decreased, confirming the molecular weight increase and the complex formation (Figure 7). From the graph, the binding constant between β-CD–MCM–CP and FITC-hex-ADM was calculated to be 1.49×10^4 M^{-1}.

Furthermore, 2D ROESY NMR experiment was performed to show the formation of the inclusion complex. Figure 8(a and b) exhibit the ROESY spectra of the β-CD/FITC-hex-ADM and β-CD–MCM–CP/FITC-hex-ADM mixtures, respectively. The α, β and γ protons of the adamantane in FITC-hex-ADM showed strong cross-peaks by interaction with the H3, H5 and H6 protons in the cavity of native β-CD, and weaker cross-peaks by interaction with the H2 and H4 protons on the exterior of the β-CD cavity (Figure 8a). Similarly, the cross-peaks between the protons of the adamantane derivatives and β-CD–MCM–CP were also observed (Figure 8b). The spectra represent the spatial proximity at the 5 Å maximal limit among the protons of β-CD derivatives and the adamantane moiety. Both data strongly indicate complex formation between β-CD–MCM–CP and FITC-hex-ADM.

Cytotoxicity

The short-term biocompatibility of the β-CD–MCM drug carrier was preliminarily checked by MTT assay on NIH3T3 cells (Figure 9). Branched polyethylenimine 25 kDa, a well-known polymeric drug delivery carrier with high cytotoxicity, was used as a positive control. Up to 100 μM, β-CD, β-CD–MCM and β-CD–MCM–CP exhibited almost no cytotoxicity until 48 h.

Discussion

In this study, we intended to develop a pH-sensitive drug carrier that could sense the small pH drop from 7.4 to 5.5 and rapidly release the conjugated drug molecules. A backbone with many conjugating residues was preferred for high drug contents. In addition, various functions can be introduced by a simple method for a multi-role drug delivery carrier. We selected β-CD as the backbone of the carrier due to high biocompatibility [20], modifiability of many hydroxyl groups [24] and strong non-covalent complex formation with adamantane [27]. As a pH-sensitive linker, we selected a maleic acid amide derivative because it can be easily synthesised by the simple mixing between the corresponding

Figure 4. Release of BA from β-CD–MCM–BA at acidic pH measured by ^{1}H NMR (NMR solvent: D_2O).

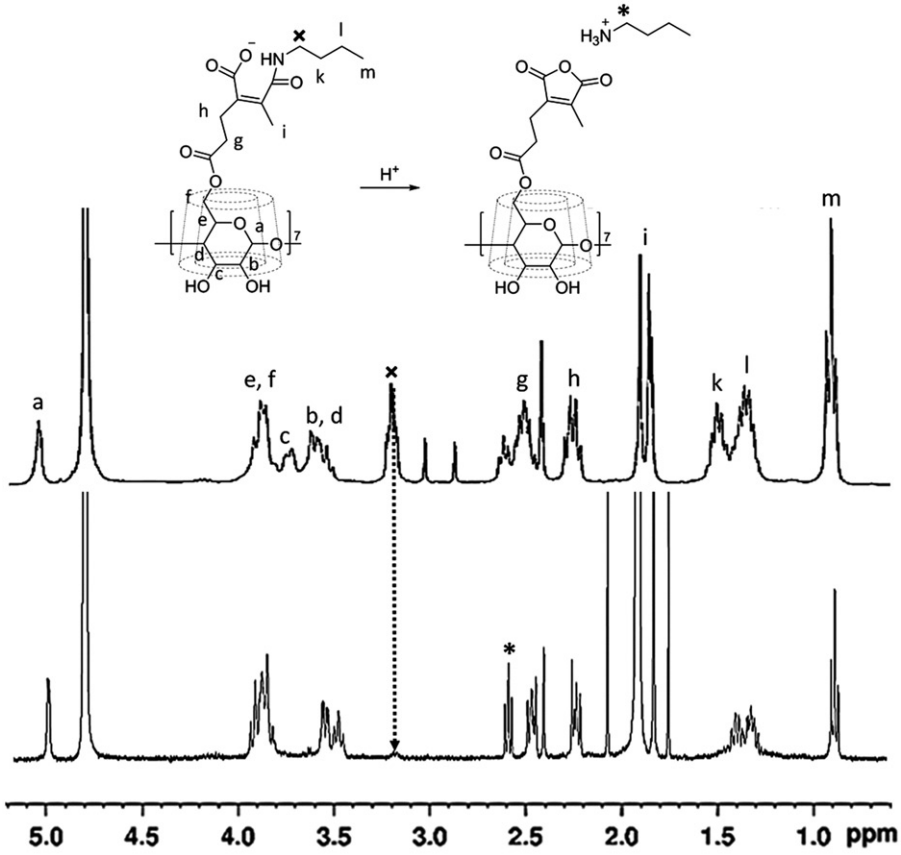

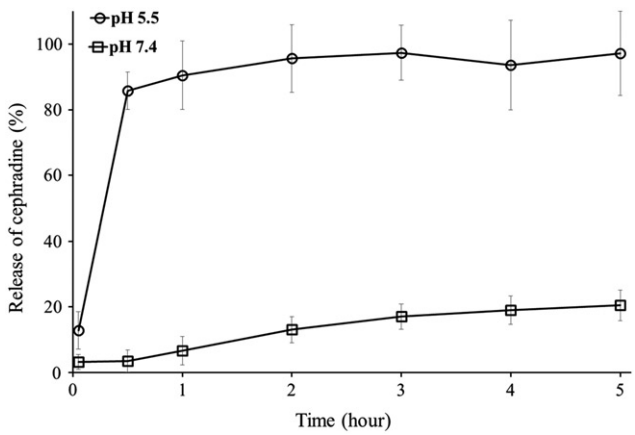

Figure 5. pH-responsive release of CP from β-CD–MCM–CP at pH 5.5 (acetate buffer, 100mM; ○) and pH 7.4 (phosphate buffer, 100 mM; □) measured by HPLC. The error bar represents the standard deviation ($n = 3$).

anhydride and amine and it shows pH-dependent degradability. A maleic acid amide derivative has a *cis*-β-carboxylate group that can internally attack the carbonyl group of the amide *via* five-membered ring formation, and it shows much higher vulnerability than a simple amide [20,35]. The pH-sensitivity is also dependent upon the alkyl substituent on the *cis*-double bond. Bulkier substituents can accelerate the internal attack of the β-carboxylate group to increase the degradability at weakly acidic pH [36]. Among various maleic acid amide derivatives, we selected the MCM acid amide because it showed rapid degradability at pH 5.5 owing to the methyl and carboxyethyl substituents [22,37,38].

We successfully synthesised β-CD–MCM *via* a one-step reaction by the carbodiimide coupling method using DIC (Figure 2) under catalysts of DMAP and PTSA. Although coupling reactions of MCM using thionyl chloride ($SOCl_2$) or oxalyl chloride were reported previously [39], they showed significant side reactions in the coupling between β-CD and MCM, so we selected the DIC coupling method to achieve a high yield of the product. The addition of both DMAP and PTSA could facilitate the ester formation without the formation of side products including *N*-acylurea in polar solvents [40]. We could control the numbers of MCM residues that coupled to β-CD by adjusting the amount of reactants, and consequently obtain a ''medusa-like'' β-CD–MCM with six MCM residues on average, which was confirmed by ^{1}H NMR and mass spectroscopy (Figure 3). Because the face of the secondary hydroxyl groups in β-CD readily interacts with an adamantane guest molecule [41], the medusa-like structure by the modification of primary hydroxyl group would be preferred for the future inclusion of a functional moiety.

We expected a high efficiency in the drug conjugation with β-CD–MCM because the anhydride group of MCM is very reactive with nucleophiles such as primary amines in alkaline conditions, even if the nucleophilic attack is interfered with by steric hindrance. In both cases of β-CD–MCM–BA and β-CD–MCM–CP, we similarly observed high drug efficiency, with the values of 90% and 92.5% for BA and CP, respectively. By the covalent conjugation with β-CD–MCM, the drugs can avoid premature release from the drug delivery carrier in the diluted concentrations in physiological fluids.

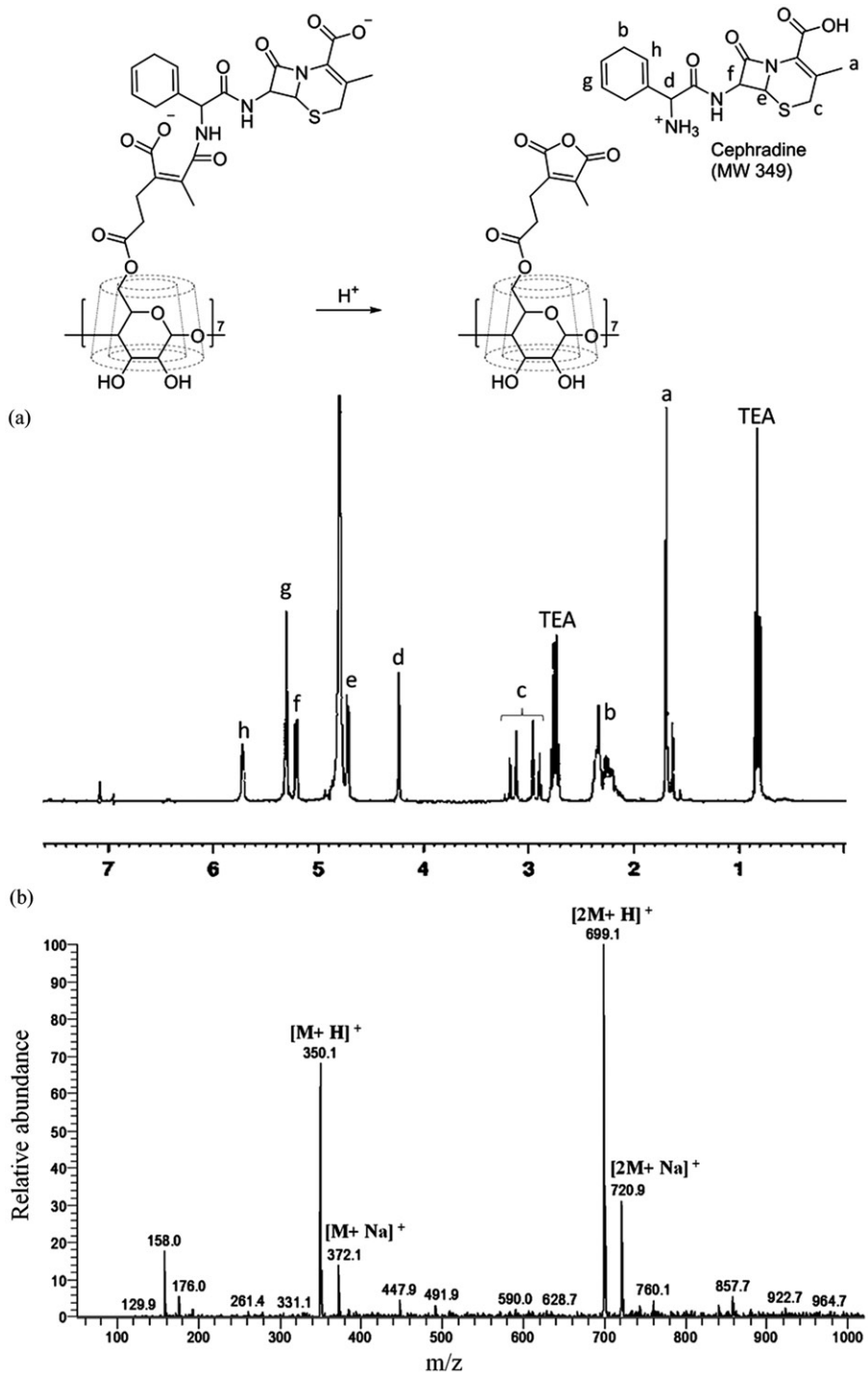

Figure 6. Identification of the released CP from β-CD–MCM–CP. (a) ^{1}H NMR (NMR solvent: D_2O) and (b) ESI mass spectra of the released CP.

We investigated the drug-release kinetics of β-CD–MCM–CP at pH 5.5 and pH 7.4. Remarkably, CP was dramatically released from β-CD–MCM at pH 5.5 up to 80% within 0.5 h and 95% within 1 h, while it was barely released at pH 7.4 (Figure 5). The chemical stability of CP during the conjugation and release was also secured. On the basis of the delicate sensing of the small pH difference and the outstanding release kinetics at the weakly acidic pH, we believe that β-CD–MCM can be used as a drug carrier for targeting tumours, inflammatory tissues or abscesses as well as for early endosomal escape in intracellular drug delivery. β-CD–MCM–CP enables the delivery of antibiotics into pneumonia or other inflamed tissues specifically, to avoid side effects and overdoses.

As mentioned above, β-CD is a cyclic oligosaccharide composed of seven-membered α-D-glucopyranoside units linked 1 to 4, and it contains a less hydrophilic interior space and a more hydrophilic outer surface. This allows β-CD to form inclusion complexes with various molecules through host-guest interactions. Adamantane, a cycloalkane consisting of four connected cyclohexane rings, is the most representative guest molecule for β-CD. Therefore, we can introduce a functional moiety such as a targeting ligand or a cell penetrating peptide into β-CD–MCM by the tethering of an adamantane residue in the functional moiety and the simple mixing with β-CD–MCM. For the confirmation of this concept, we synthesised a FITC-labelled adamantane derivative to trace the inclusion complex by FCS. The diffusion

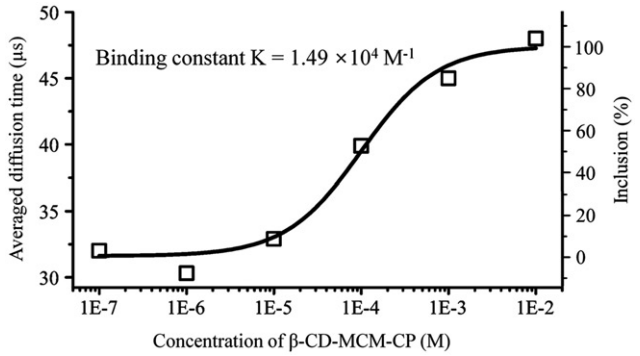

Figure 7. Variation of the average diffusion time measured by FCS to confirm the complex formation between β-CD–MCM–CP and FITC-hex-ADM.

coefficient of the fluorophore was decreased significantly due to the complex formation. The binding constant was calculated from the ''S''-type curve between the diffusion time and the concentration of β-CD–MCM (Figure 7). The binding constant K was 1.49×10^4 M^{-1}, meaning the interaction between β-CD–MCM–CP and the adamantane derivative was similar to the general β-CD/adamantane host–guest interaction because the general association constant K is $1–10 \times 10^4$ M^{-1} [42]. Based on the binding constant, the inclusion percentage could also be calculated and be shown in Figure 7. The host–guest inclusion between β-CD–MCM–CP and adamantane derivative was further confirmed by ROESY spectra (Figure 8). Strong cross-peaks in β-CD–MCM–CP/FITC-hex-ADM were comparable with those of β-CD/FITC-hex-ADM. The medusa-like conjugation of six MCM molecules in the face of primary hydroxyl groups did not affect the inclusion significantly. Based on these results, any functional moieties could be introduced into β-CD–MCM after the drug conjugation by the formation of the inclusion complex. Of course, other drug carriers such as polymers or nanoparticles with adamantane moieties can be easily modified with β-CD–MCM through the host–guest interaction for pH-sensitive conjugation of drugs or other functionalities.

Finally, we verified that β-CD–MCM and its drug conjugate showed almost no sign of acute cytotoxicity up to 100 μM in a eukaryotic cell line by MTT assay (Figure 9), although the long-term toxicity and bioadaptability should be analysed by various methods in the future.

As a novel drug-conjugating system, β-CD–MCM has great advantages in easy conjugation of drugs and multi-functionalities as well as rapid release of drugs responding to small pH drop. CP, an antibiotic model drug in this research, can be specifically delivered into bacteria-infected sites by a β-CD–MCM-based drug carrier. β-CD–MCM, with a molar mass of several thousands, can be used as a pH-sensitive drug carrier by itself for a site-specific delivery of drugs into weakly acidic targets such as tumours, abscesses or inflammatory tissues. For longer circulation or enhanced permeability and retention effect, β-CD–MCM can be introduced into other drug delivery carriers with several hundred nanometres by non-covalent interactions. The future animal study will be followed for the proof of the specificity and efficacy of β-CD–MCM-based drug delivery systems.

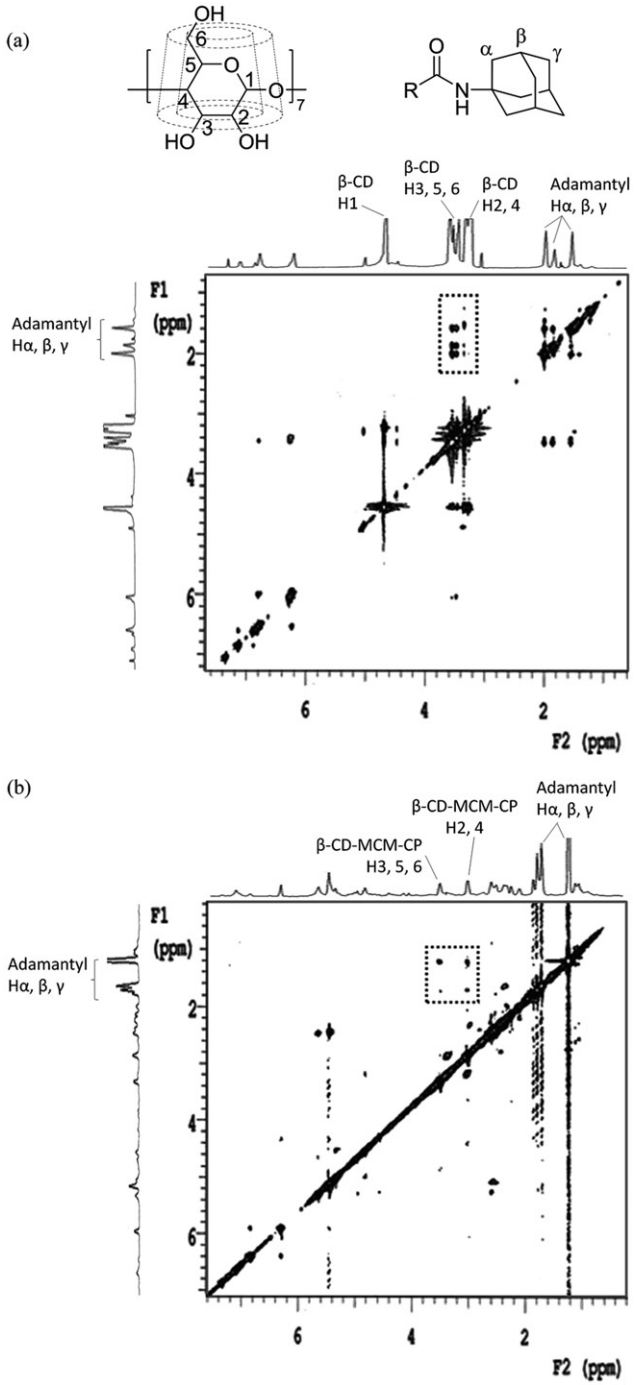

Figure 8. Expansion of NMR 2D ROESY (NMR solvent: D_2O) spectra of the inclusion complex between (a) β-CD and FITC-hex-ADM and (b) β-CD–MCM–CP and FITC-hex-ADM.

Conclusion

We successfully developed a novel drug delivery carrier, β-CD–MCM, which has a rapid release profile in response to a small pH drop. β-CD–MCM possesses several ready-to-use anhydride residues for simple and almost exhaustive conjugation with amine-containing drugs. β-CD–MCM–CP, one of the drug conjugates, exhibited a remarkable capability to discriminate between pH 7.4 and 5.5 to release the conjugate antibiotic. Moreover, the internal cavity of β-CD–MCM–CP is easily accessible for complexation with other functional groups with an adamantane residue. Based on these attractive

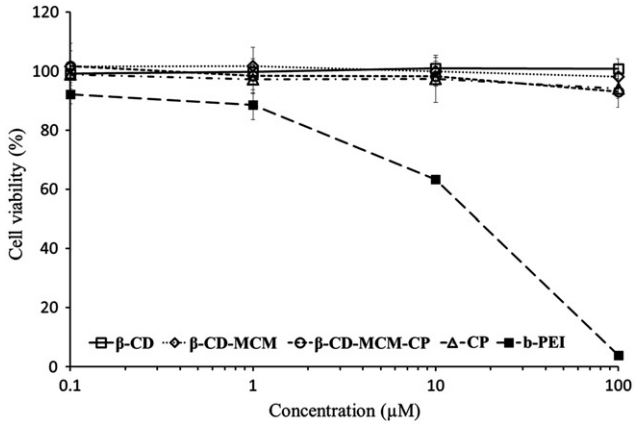

Figure 9. Cytotoxicity in NIH3T3 cells of β-CD (□), β-CD–MCM (◇), β-CD–MCM–CP (○), CP (△) and PEI (■). Each error bar represents the standard deviation ($n = 3$).

characteristics, β-CD–MCM has great potential as a multi-functional drug delivery carrier for targeting tissues or organelles with weakly acidic pH conditions.

Acknowledgements

This paper is dedicated to my respectable mentor, Prof Kazunori Kataoka.

Declaration of interest

The authors report no declarations of interest.

This work was supported by the Seoul R&BD program (ST110017M0209721); the Basic Science Research Program (NRF-2010-0007118) of the National Research Foundation funded by the Ministry of Education, Science and Technology of Korea; the Mid-Career Researcher Program (NRF-2011-0013569) from the Ministry of Science, ICT and Future Planning, Korea; and the GAIA project (2013000550004) funded by the Ministry of Environment, Korea.

References

1. Fleige E, Quadir MA, Haag R. Stimuli-responsive polymeric nanocarriers for the controlled transport of active compounds: concepts and applications. Adv Drug Delivery Rev 2012;64:866–84.
2. Lee Y, Kataoka K. Biosignal-sensitive polyion complex micelles for the delivery of biopharmaceuticals. Soft Matter 2009;5:3810–17.
3. Gupta P, Vermani K, Garg S. Hydrogels: from controlled release to pH-responsive drug delivery. Drug Discovery Today 2002;7:569–79.
4. Prasannan A, Tsai H-C, Chen Y-S, Hsiue G-H. A thermally triggered in situ hydrogel from poly(acrylic acid-co-N-isopropylacrylamide) for controlled release of anti-glaucoma drugs. J Mater Chem B 2014;2:1988–97.
5. Jiang J, Tong X, Zhao Y. A new design for light-breakable polymer micelles. J Am Chem Soc 2005;127:8290–1.
6. Lee Y, Fukushima S, Bae Y, et al. A protein nanocarrier from charge-conversion polymer in response to endosomal pH. J Am Chem Soc 2007;129:5362–3.
7. Cheng R, Feng F, Meng F, et al. Glutathione-responsive nanovehicles as a promising platform for targeted intracellular drug and gene delivery. J Controlled Release 2011;152:2–12.
8. Miyata T, Uragami T, Nakamae K. Biomolecule-sensitive hydrogels. Adv Drug Delivery Rev 2002;54:79–98.
9. Gao W-W, Chan JM, Farokhzad OC. pH-responsive nanoparticles for drug delivery. Mol Pharmaceutics 2010;7:1913–20.
10. Wu XL, Kim JH, Koo H, et al. Tumor-targeting peptide conjugated pH-responsive micelles as a potential drug carrier for cancer therapy. Bioconjugate Chem 2010;21:208–13.
11. Punnia-Moorthy A. Evaluation of pH changes in inflammation of the subcutaneous air pouch lining in the rat, induced by carrageenan, dextran and *Staphylococcus aureus*. J Oral Pathol Med 1987;16:36–44.
12. Bessman AN, Page J, Thomas LJ. In vivo pH of induced soft-tissue abscesses in diabetic and nondiabetic mice. Diabetes 1989;38:659–62.
13. Ford C, Hamel J, Stapert D, Yancey R. Establishment of an experimental model of a *Staphylococcus aureus* abscess in mice by use of dextran and gelatin microcarriers. J Med Microbiol 1989;28:259–66.
14. Abhay A, Singh CA, Vamanrao DP, Kumar JN. Poly(amidoamine) (PAMAM) dendritic nanostructures for controlled site-specific delivery of acidic anti-inflammatory active ingredient. AAPS PharmSciTech 2005;6:E536–42.
15. Lee Y, Miyata K, Oba M, et al. Charge-conversion ternary polyplex with endosome disruption moiety: a technique for efficient and safe gene delivery. Angew Chem Int Ed 2008;47:5163–6.
16. Rozema DB, Lewis DL, Wakefield DH, et al. Dynamic PolyConjugates for targeted in vivo delivery of siRNA to hepatocytes. PNAS 2007;104:12982–7.
17. Lee Y, Ishii T, Cabral H, et al. Charge-conversional polyionic complex micelles-efficient nanocarriers for protein delivery into cytoplasm. Angew Chem Int Ed 2009;48:5309–12.
18. Mellman I, Fuchs R, Helenius A. Acidification of the endocytic and exocytic pathways. Annu Rev Biochem 1986;55:663–700.
19. Lee Y, Ishii T, Kim HJ, et al. Efficient delivery of bioactive antibodies into the cytoplasm of living cells by charge-conversional polyion complex micelles. Angew Chem Int Ed 2010;49:2552–5.
20. Kirby AJ, Lloyd GJ. Structure and efficiency in intramolecular and enzymic catalysis: intramolecular general base catalysis. Catalysis of amide hydrolysis by the carboxy-group of substituted maleamic acids. J Chem Soc Perkin Trans 2 1976:1753–61.
21. Mehta NB, Phillips AP, Lui FF, Brooks RE. Maleamic and citraconamic acids, methyl esters, and imides. J Org Chem 1960;25:1012–15.
22. Rozema DB, Ekena K, Lewis DL, et al. Endosomolysis by masking of a membrane-active agent (EMMA) for cytoplasmic release of macromolecules. Bioconjugate Chem 2003;14:51–7.
23. Davis ME, Brewster ME. Cyclodextrin-based pharmaceutics: past, present and future. Nat Rev Drug Discovery 2004;3:1023–35.
24. Cravotto G, Bicchi C, Tagliapietra S, et al. New chiral selectors: design and synthesis of 6-TBDMS-2,3-methyl beta-cyclodextrin 2-2′ thioureido dimer and 6-TBDMS-2,3-methyl (or 2-methyl-3-acetyl) beta-cyclodextrin bearing an (R) Mosher acid moiety. Chirality 2004;16:526–33.
25. Motoyama K, Onodera R, Okamatsu A, et al. Potential use of the complex of doxorubicin with folate-conjugated methyl-beta-cyclodextrin for tumor-selective cancer chemotherapy. J Drug Targeting 2014;22:211–19.
26. Copolovici DM, Langel K, Eriste E, Langel U. Cell-penetrating peptides: design, synthesis, and applications. ACS Nano 2014;8:1972–94.
27. Hakkarainen B, Fujita K, Immel S, et al. 1H NMR studies on the hydrogen-bonding network in mono-altro-beta-cyclodextrin and its complex with adamantane-1-carboxylic acid. Carbohydr Res 2005;340:1539–45.
28. Kulkarni A, Deng W, Hyun SH, Thompson DH. Development of a low toxicity, effective pDNA vector based on noncovalent assembly of bioresponsive amino-beta-cyclodextrin:adamantane-poly(vinyl alcohol)-poly(ethylene glycol) transfection complexes. Bioconjugate Chem 2012;23:933–40.
29. Naganawa A, Ichikawa Y, Isobe M. Synthetic studies on tautomycin. Synthesis of 2,3-disubstituted maleic anhydride segment. Tetrahedron 1994;50:8969–82.
30. Humblet V, Misra P, Bhushan KR, et al. Multivalent scaffolds for affinity maturation of small molecule cell surface binders and their Application to Prostate Tumor Targeting. J Med Chem 2009;52:544–50.

31. Petrasek Z, Schwille P. Precise measurement of diffusion coefficients using scanning fluorescence correlation spectroscopy. Biophys J 2008;94:1437–48.
32. Kim SA, Heinze KG, Schwille P. Fluorescence correlation spectroscopy in living cells. Nat Methods 2007;4:963–73.
33. Granadero D, Bordello J, Perez-Alvite MJ, et al. Host-guest complexation studied by fluorescence correlation spectroscopy: adamantane-cyclodextrin inclusion. Int J Mol Sci 2010;11:173–88.
34. Smirnov D, Dhall A, Sivanesam K, et al. Fluorescent probes reveal a minimal ligase recognition motif in the prokaryotic ubiquitin-like protein from *Mycobacterium tuberculosis*. J Am Chem Soc 2013; 135:2887–90.
35. Suh J, Baek D-J. Intramolecular catalysis of amide hydrolysis by carboxyl and metal ion/proton agents. I. Intramolecular reactions of imidazole or pyridine derivatives of maleamic acid. Bioorg Chem 1981;10:266–76.
36. Kirby AJ, McDonald RS, Smith CR. Intramolecular catalysis of amide hydrolysis by two carboxy groups. J Chem Soc Perkin Trans 2 1974:1495–504.
37. Monahan SD, Subbotin VM, Budker VG, et al. Rapidly reversible hydrophobization: an approach to high first-pass drug extraction. Chem Biol 2007;14:1065–77.
38. Takemoto H, Miyata K, Hattori S, et al. Acidic pH-responsive siRNA conjugate for reversible carrier stability and accelerated endosomal escape with reduced IFNalpha-associated immune response. Angew Chem Int Ed 2013;52:6218–21.
39. Wong SC, Wakefield D, Klein J, et al. Hepatocyte targeting of nucleic acid complexes and liposomes by a T7 phage p17 peptide. Mol Pharmaceutics 2006;3:386–97.
40. Moore JS, Stupp SI. Room temperature polyesterification. Macromolecules 1990;23:65–70.
41. Li L, Guo X, Wang J, et al. Polymer networks assembled by host-guest inclusion between adamantyl and β-cyclodextrin substituents on poly(acrylic acid) in aqueous solution. Macromolecules 2008; 41:8677–81.
42. Harries D, Rau DC, Parsegian VA. Solutes probe hydration in specific association of cyclodextrin and adamantane. J Am Chem Soc 2005;127:2184–90.